

1
2
3
4
5
6
7
8
9
10
11
12
13
14
15
16
17
18
19
20
21
22
23

Modeling larval dispersal and connectivity for Atlantic sea scallop (*Placopecten magellanicus*) in the Middle Atlantic Bight

Daphne M. Munroe^{1,2}, Dale Haidvogel², Joseph C. Caracappa^{1,2}, John M. Klinck³, Eric N. Powell⁴, Eileen E. Hofmann³, Burton V. Shank⁵, Deborah R. Hart⁵

1. Haskin Shellfish Research Laboratory, Rutgers University, Port Norris, NJ, USA
2. Department of Marine and Coastal Science, Rutgers University, New Brunswick, NJ, USA
3. Center for Coastal Physical Oceanography, Old Dominion University, Norfolk, VA, USA
4. Gulf Coast Research Laboratory, The University of Southern Mississippi, Ocean Springs, MS, USA
5. NMFS Northeast Fisheries Science Center 166 Water St. Woods Hole, MA, USA

ABSTRACT: Larval Atlantic sea scallops (*Placopecten magellanicus*) simulations in the Middle Atlantic Bight (MAB) from 2006-2012 were performed to investigate annual and inter-annual dispersal and connectivity patterns among stock regions. These simulations used a circulation model based on the Regional Ocean Modeling System (ROMS) and an individual-based larval model (IBM) that included larval behavior. The circulation model used realistic dynamical forcing (e.g., winds, tides, and open ocean boundary conditions), thermo-dynamical fluxes (e.g.,

24 solar radiations, sensible and latent heating), and hydrological forcing; the larval IBM included
25 vertical swimming and sinking behaviour, temperature-dependent growth, and settlement.
26 Simulated larvae that reach settlement size and suitable habitat in 45 days are considered
27 ‘successful’, and two regions are considered ‘connected’ by larval dispersal when larvae
28 successfully disperse from one region to the other. In general, simulated larval dispersal patterns
29 varied seasonally (28% higher in September and October compared to May and June), among
30 years (2007 through 2009 had 5% lower larval success during August and September compared
31 to other years), and spatially, with larvae released from the northern regions like Long Island
32 acting as a substantive larval source with 14% greater dispersal success and 15% greater
33 connectivity with other regions than those released elsewhere. Over the seven years simulated,
34 the MAB scallop stocks showed high rates of connectivity to regions to the south and more
35 limited and variable connectivity to regions to the north. In species like sea scallops with limited
36 adult mobility, larval dispersal supplies recruits, enables range expansion, and connects
37 populations. Thus, appreciation of dispersal patterns are essential for fishery management of this
38 economically valuable stock.

39

40 **1. Introduction**

41 Larval dispersal is important to understanding population dynamics (Possingham &
42 Roughgarden, 1990; Pineda et al., 2007; Kerr et al., 2010; Munroe & Noda, 2010; Munroe et al.,
43 2012), genetic connectivity (Schetema, 1971; Munroe et al., 2015), and species range shifts
44 (Zhang et al., 2015) in most marine invertebrates. This is particularly true for widely distributed,
45 benthic species with limited adult mobility and long-duration planktotrophic larval stages, such
46 as Atlantic sea scallops (*Placopecten magellanicus*). Larval dispersal brings the next generation

47 of recruits into the overall population, is the mechanism by which range expansion can occur,
48 and is the conduit by which different parts of sessile populations connect or mix with one another.
49 Therefore, understanding larval dispersal and connectivity patterns within the larger population
50 may be essential for fishery management (Kritzer and Sale, 2004) and predicting impacts of
51 future climatic and oceanographic changes on species range distributions (Bernhardt & Leslie,
52 2013).

53 Simulation studies that include tracking of passive particles show that the Middle Atlantic
54 Bight (MAB) shelf circulation can potentially disperse shellfish larvae hundreds of kilometers
55 from their natal origins (Zhang et al., 2015). However, most marine larvae exhibit behavior, such
56 as vertical swimming oriented to particular depths or conditions, and inclusion of this behavior
57 with heterogeneous oceanographic currents has been shown to result in shorter dispersal and
58 more retentive conditions (Metaxas, 2001; Metaxas and Saunders, 2009; Strathmann et al., 2002).
59 Furthermore, larval growth and swimming are important components of larval dispersal models
60 because behavior has been demonstrated to be important in determining dispersal distance,
61 settlement success, and overall connectivity patterns (e.g., Xue et al., 2008; North et al., 2008;
62 Tian et al., 2009; Kim et al., 2010; Narváez et al., 2012a,b; Zhang et al., 2015). The extent of
63 larval dispersal away from or retention closer to their birthplace are important considerations for
64 understanding the overall metapopulation structure in commercial fisheries for many shellfish
65 and potentially other species with limited adult mobility (Kritzer and Sale, 2004).

66 The U.S. Atlantic sea scallop (*Placopecten magellanicus*) fishery is among the most
67 valuable fisheries in the U.S., with an ex-vessel value in excess of \$486 million USD in 2016
68 (NMFS, 2017). This fishery has shown a remarkable recovery from a severely overfished state in
69 the early 1990s. Scallop biomass increased twelve-fold between 1994 to 2009, while landings

70 more than tripled (NEFSC, 2014). Though these increases are due to a combination of
71 management measures and ecological factors (Hart & Rago, 2006; Shank et al., 2012),
72 implementation of a rotation management program is viewed as an important contributor. In the
73 U.S. scallop fishery management program, these rotational area closures are applied in part to
74 stabilize and enhance the scallop population by preventing fishing on abundant cohorts of small
75 scallops, allowing them to grow and reproduce in highly dense aggregations before they reach
76 appropriate size for the fishery. An important mechanism underlying the success of such a
77 strategy is larval supply (spillover) from high abundance regions or rotational closures to the
78 wider stock. Sea scallop recruitment in the MAB is positively correlated with regional stock
79 biomass, which suggests that increased larval supply tends to result in higher recruitment (Hart
80 2013, NEFSC 2014). Similarly, recruitment of bay scallops (*Argopecten irradians*) in Peconic
81 Bay improved following increases in the adult stock size (Tettlebach et al., 2013; see also
82 Peterson et al., 1996).

83 Atlantic sea scallops are known to spawn in the spring (May), with a second spawn in the
84 fall (DuPaul et al., 1989; Schmitzer et al., 1991). Additionally, larval scallops have been the
85 focus of laboratory studies and field surveys and much is known about larval swimming behavior
86 and vertical distribution in the water column (Tremblay & Sinclair, 1990; Manuel et al., 1996;
87 Gilbert et al., 2010), response to temperature (Tremblay & Sinclair 1988, 1990; Manuel et al.,
88 2000; Pearce et al., 2004), and growth (Hurley et al., 1986; Manuel & Dadswell 1991,1993;
89 Pernet 2003; Gallagher et al., 1996). These behaviors and how they interact with heterogeneous
90 oceanographic conditions throughout the spawning period and across the species' range underlie
91 patterns of connectivity that are important for understanding long-term population dynamics
92 (Bryan-Brown et al., 2017). Moreover, a better understanding of larval dispersal among scallop

93 stock regions (e.g. among rotational management areas or areas of high stock abundance) would
94 help to improve overall management of the species and the fishery.

95 In this study, a coupled bio-physical individual-based model is implemented to estimate
96 the patterns of connectivity among Atlantic sea scallop stock regions. Using this model, we
97 quantify the inter-annual variability in dispersal and connectivity among broad management
98 areas over seven years (2006-2012). The coupled model and dispersal simulation (connectivity)
99 results are discussed in terms of their importance for understanding the ecology of the species
100 and for management of this valuable fishery.

101

102 **2. Model implementation**

103 2a. Circulation model

104 The circulation model used in this study is an implementation of the Regional Ocean
105 Modeling System (ROMS, www.myroms.org; Shchepetkin and McWilliams, 2005) that was
106 configured to simulate circulation on the MAB. Larval particle models that consider bivalve
107 growth, development, and larval transport have been included in previous ROMS
108 implementations (e.g., Narváez et al., 2012a.b; Zhang et al., 2015; Zhang et al., 2016). For this
109 study, a larval individual-based model (IBM) for the Atlantic sea scallop as described in section
110 2b is embedded in the ROMS circulation model.

111 The coupled ROMS-IBM for a MAB model domain covering 68–77° W and 33.8–42° N
112 (Fig. 1), with 130×80 cells and 5–8 km horizontal resolution, and actual bathymetry with a
113 minimum depth set to 5 m. Vertical resolution is provided by 36 layers that are non-uniformly
114 distributed vertically such that more layers are used to increase resolution near the sea surface
115 where temperature and currents have larger vertical gradients. The time step was set to 4 hours

116 (240 minutes), with the barotropic integration every 8 seconds. ROMS settings also used fourth-
117 order centered vertical advection of momentum, fourth-order Akima horizontal advection of the
118 tracer fields (temperature and salinity), turbulent mixing using the Generic Length Scale scheme
119 (Umlauf and Burchard, 2003), and k-kl closure parameters (Mellor and Yamada, 1982).

120 The coupled ROMS-IBM model was forced every 3 hours at the sea surface by
121 atmospheric condition data (i.e., solar radiation, winds, rain, air temperature, pressure, and
122 moisture) obtained from the North American Regional Reanalysis dataset (NARR,
123 <http://www.emc.ncep.noaa.gov/mmb/rrean/>). Tidal elevation and current data for the MAB were
124 obtained from the Advanced Circulation Model ([http://adcirc.org/products/adcirc-tidal-](http://adcirc.org/products/adcirc-tidal-databases/)
125 [databases/](http://adcirc.org/products/adcirc-tidal-databases/)) and input at the model domain perimeter. Daily river transport data from the U.S.
126 Geological Survey is input into the MAB region at seven major rivers (Connecticut, Hudson,
127 Delaware, Susquehanna, Potomac, Choptank and James). Open boundary segments use radiation
128 boundary conditions (Marchesiello et al., 2001) and salinity and temperature are treated using a
129 zero-gradient condition. Along the open boundaries, the circulation model is nudged to corrected
130 and validated tracer and momentum fields from a high-resolution (1/12 degree) global simulation
131 (Wilkin and Hunter, 2013; Zhang et al., 2015). In each year, the model was run for three months
132 prior to larval release to allow for adjustment of the circulation and tracer fields.

133 2b. Larval IBM

134 The IBM is based on an established coupled modeling platform developed to simulate
135 dispersal of surfclam larvae in the MAB (Zhang, et al., 2015; Zhang et al., 2016), and dispersal
136 of oyster larvae in the Delaware Bay (Narváez et al. 2012a,b; Munroe et al. 2012, 2013). In this
137 case, the IBM simulates growth and swimming for Atlantic sea scallop larvae and is embedded
138 in the circulation model so that high-frequency dynamical processes act on larval transport and

139 dispersion.

140 Unlike many other bivalves that release eggs and sperm into the water column where
141 fertilization occurs, fertilized scallop eggs are benthic and remain on the seabed for
142 approximately one day as the embryo develops. The day-old trochophore stage enters the water
143 column (Culliney 1974; Tremblay et al., 1994); therefore, the larval model is initialized with
144 trochophores that are 1.5 days old with a size of 75 μm (Culliney 1974, Table 1).

145 Once the scallop larvae move into the water column, growth is simulated as a function of
146 temperature. Scallop larval growth at 13°C (grown under optimal laboratory conditions) was set
147 to the average slope of linear growth functions for larval scallops obtained from experimental
148 studies (Pernet et al., 2003; Gallagher et al., 1996; Gouda et al., 2006; Hurley et al., 1986; Hurley
149 et al., 1987). This relationship is used as the base growth rate at 13 °C (Gr_0), and a temperature
150 relationship was applied such that growth is zero at 0 °C, maximal at 17 °C, and decreases to
151 zero at 19 °C, following results from incubation experiments (Culliney, 1974). Growth (change
152 in length, L) over time (t) at a given temperature (T) is defined as:

153
$$\frac{dL}{dt} = Gr_0 Gr_T(T). \quad (1)$$

154

155 with $Gr_T(T)$ modifying the base growth rate for $T \leq T_2$ by:

156
$$Gr_T = \exp(Gr_1(T - T_1)), \quad (2)$$

157 and for $T > T_2$ by:

158
$$Gr_T = \max\left[0, T_{GrP} \frac{T_3 - T}{T_3 - T_2}\right] \quad (3)$$

159 where:

160
$$T_{GrP} = \exp(Gr_1(T_2 - T_1)). \quad (4)$$

161 All parameter definitions and values used are provided in Table 1.

162 Net self-directed larval movement is a result of the combination of upward swimming,
 163 downward swimming, and sinking (larval scallops sink when their shell valves are closed). The
 164 speed of larval swimming is assumed to be 0.20 mm sec^{-1} for a $250 \mu\text{m}$ veliger, an average based
 165 on helical trajectories reported in Gallagher et al. (1996). This rate is then modified by larval size,
 166 which is a function of temperature (Table 1). The amount of time spent swimming upward versus
 167 downward follows a hyperbolic tangent function such that at temperatures below $\sim 14.5^\circ\text{C}$ larvae
 168 will swim almost exclusively upward. A 50:50 balance of upward and downward swimming is
 169 assumed at 16.5°C , and at temperatures above $\sim 18^\circ\text{C}$ larvae swim downward almost exclusively.
 170 Sinking rates of scallop larvae are based on reported values (Beaumont and Barnes, 1992; Chia
 171 et al., 1984; Gallagher et al. 1996) and change based upon the size of the larvae. At any given
 172 time, larvae can either swim or sink, and their activity is allocated so that 92% of the time they
 173 will swim and will sink 8% of the time; this parameter was set to allow simulated vertical
 174 distributions to match observations showing orientation within the pycnocline (Gilbert et al.,
 175 2010; Tremblay and Sinclair, 1990). In combination, these upward swimming (U_{S_s}), downward
 176 swimming (D_{S_s}), and sinking (Sk) behaviors result in net larval movement that tends to be
 177 upward in temperatures less than $\sim 16^\circ\text{C}$ and downward in temperatures greater than $\sim 16^\circ\text{C}$.
 178 Varying the dependency of swimming and sinking on larval size means that net movement varies
 179 ontogenetically with larvae $>240\mu\text{m}$ tending to move downward to the seabed for settlement.

180 The vertical movement (dZ) of larvae over time (t) is given as:

$$181 \quad \frac{dZ}{dt} = -Sk(L)(1 - Fu(T)) + (U_{S_s}(L) \times Fu(T)) - D_{S_s}(L)(1 - Fu(T)) \quad (5)$$

182 where passive sinking (Sk) varies with length (L) as:

$$183 \quad Sk(L) = Sk_0 L^{Sk_1}, \quad (6)$$

184 upward swimming speed (U_{S_s}) varies with length (L) as:

185
$$U_{S_s}(L) = U_{S_0} + U_{S_1}L + U_{S_2}L^2 , \quad (7)$$

186 and downward swimming speed (D_{S_s}) varies with length (L) as:

187
$$D_{S_s}(L) = D_{S_0} + D_{S_1}L + D_{S_2}L^2 . \quad (8)$$

188 The fraction of time swimming upward (Fu_s) varies with temperature (T) such that:

189
$$Fu(T) = Fu_{s0} \left(1 - \tanh \left(\frac{(T - T_{us1})}{T_{us2}} \right) \right) \quad (9)$$

190 All parameter definitions and values used are provided in Table 1.

191 Scallop larvae are competent to metamorphose at shell sizes greater than 220 μm and
 192 have been observed to settle approximately 35 days post-hatch (Culliney, 1974), with the
 193 potential to delay metamorphosis or extend larval duration (Culliney, 1974; Gallagher et al.,
 194 1996; Pearce et al, 2004). Thus, simulated larvae were assumed to settle (i.e., transition from a
 195 pelagic dispersive particle to a stationary bottom particle) when they reach a shell length >250
 196 μm and encounter suitable seabed habitat (defined by depth and adult distribution). Once the
 197 settlement length (250 μm) is reached, simulated larvae settle to the seabed at their existing
 198 horizontal location and remain fixed. Larvae that reach settlement length in 45 days and are in
 199 one of the five designated regions are considered ‘successful’. Any of the following conditions
 200 result in ‘unsuccessful’ (nonviable) larvae: failure to reach settlement size within 45 days,
 201 settlement at a depth greater than 100 m, settlement outside the designated habitat, or larvae that
 202 leave the model domain. Two regions are considered ‘connected’ by larval dispersal when larvae
 203 successfully disperse from one region to the other.

204 Sensitivity simulations were performed to test dispersal of particles with IBM off (neutral
 205 particles without behavior). These simulations showed that passive particles were only 34% as
 206 successful as those with behavior, and that they travel only 45% as far alongshore. These results
 207 are due to the fact that without behavior, particles are unable to maintain position near the

208 thermocline and are consistent with results obtained using a similar model domain and a slightly
209 different IBM (Zhang et al., 2015). Further sensitivity simulations were performed to test
210 whether larval behavior module produced expected vertical distributions under controlled
211 (mesocom mimicing) conditions. These simulations introduced larvae into a 50 m water column,
212 with a bottom temperature of 8°C, a thermocline at ~20 m depth, and a surface temperature of
213 21°C. The larvae swam up to the thermocline in approximately 5 days and maintained their
214 position near the thermocline through day 38. At day 38 (250 µm shell length) the larvae moved
215 downward to the seabed to settle. Additional simulations tested the effects of turbulent mixing in
216 which larvae were mixed above and below the thermocline during development. Larvae abruptly
217 mixed 4 to 7 m above or below the thermocline were able to return to the thermocline within 3 to
218 5 hours of displacement. Despite displacement and mixing, larvae were able to grow to
219 settlement size within 38 to 40 days. Simulated larvae grew and moved as expected based on
220 laboratory and field observations.

221

222 2c. Simulations

223 The coupled ROMS-IBM was used to simulate physical conditions and scallop larval
224 transport for the years 2006-2012, providing seven years of simulated scallop larval dispersal in
225 the MAB. The shelf waters shallower than 100 m were separated into five regions that
226 correspond to scallop management areas (NEFSC, 2014) off Virginia Beach, Delmarva, New
227 York Bight, Long Island, and Block Island (Fig. 1). The simulated larvae were released in the
228 four southern regions, however; no larvae were released from Block Island because of low
229 spawning stock density there (Figure 1). All five regions received larvae. The total numbers of
230 larvae released from each region was scaled each year to proportionally reflect the spatially-

231 explicit observed scallop spawning biomass during that year (NEFSC, 2014). As an example, in
232 2006, a total of 3857, 14658, 31050, and 32693 larvae were released from each region (south to
233 north, regional annual release totals for each year are provided in Table 2. Larvae were released
234 on 36 days with three releases occurring at 00:00, 04:08, and 08:17 each day. Although scallops
235 tend to spawn in spring and fall, release days occurred on day 1, 6, 11, 16, 21, and 26 of May
236 through October each year for completeness of seasonal coverage.

237

238 **3. Results**

239 Success of larval dispersal varied among regions, seasonally, and by year (Figure 2,
240 Supplementary Materials). On average over all release years, the greatest larval success occurred
241 for larvae released from the northern region (Long Island) during September (Figure 2 bottom
242 right panel). On average, larvae released from Long Island had 14% greater success and 15%
243 greater connectivity than those released from southern regions. Some years show larval success
244 over a protracted range of regions and dates (e.g. 2010 and 2011, Figure 2), whereas other years
245 show a more constrained pattern of larval success over release dates and regions (e.g. 2007,
246 Figure 2). The period of 2007 through 2009 had 5% lower larval success for larvae released
247 during August and September compared to other years.

248 Simulated larval success is the combined result of differences in growth rate, which is
249 largely determined by temperature and dispersal to a habitable region. Like larval settlement
250 success, larval growth rate varied among regions, seasonally, and by year (Figure 3). On average
251 over all years, fastest rates of larval growth were observed for the southern regions (Delmarva
252 and Virginia Beach) and for the later releases in September and October (Figure 3 bottom right

253 panel). In some years, larval growth rate remained relatively high in the northern regions over a
254 protracted period of release times, from July through October (e.g. 2009, 2011, Figure 3).

255 The relationship between the median temperature experienced by a released group of
256 larvae and the average growth rate over the same group's pelagic life is relatively unimodal, with
257 an optimum at 15°C (Figure 4). Temperature and growth tend to vary seasonally, with successful
258 larvae released in the latter part of the year (September and October) experiencing relatively
259 cooler temperatures (<14°C) and high growth (3.5 to 4.0 $\mu\text{m d}^{-1}$). Whereas in May, June, and
260 July successful larvae tend to experience warmer and more variable temperatures on average and
261 have correspondingly lower and more variable growth rates (Figure 4).

262 Connectivity, a product of both larval success and oceanographic dispersal patterns, also
263 varies seasonally and by year. In general, averaging over all larval releases and all years,
264 connectivity is high among the regions, with each region supplying larvae most strongly to the
265 region south of it and retaining some of its own larvae (Fig 5). Connectivity tends to be stronger
266 when larval success is higher later in the season. Spawning occurs most consistently in
267 September for this species in the modeled region (D. Hart, unpublished data) and simulated
268 connectivity for larvae released in September shows a general downcoast pattern, with most
269 regions highly connected to the region directly to the south (Figure 6). Additionally, during the
270 first four years of the simulations with larvae released in September, the Long Island and New
271 York Bight regions supply a small percentage of larvae upstream to the region directly north
272 (Figure 6). The Long Island region is the most widely connected; in five of seven years, larvae
273 released in September from the Long Island region successfully disperse to all other regions
274 (Figure 6). In contrast, the Virginia Beach region is the least connected to other regions with four
275 of seven years having no larval dispersal to any other region (Figure 6).

276

277 **4. Conclusion and Discussion**

278 There is a general southward flow along the MAB (Lentz, 2008) which likely drives the
279 somewhat downcoast larval dispersal pattern estimated from the coupled circulation-IBM
280 simulations. The simulated patterns of connectivity among Atlantic sea scallop stock regions
281 show that, in general, larval settlement success and connectivity patterns vary seasonally (28%
282 higher in September to October compared to May to June), among years (2007 through 2009 had
283 5% lower larval success during August and September in comparison to other years), and
284 spatially with larvae released from the northern regions having greater success and connectivity
285 than those released from southern regions. These simulated patterns of variability on the scale of
286 season, year, and region are consistent with patterns described in other studies for other species
287 (Narváez et al. 2012b; Paris et al. 2007; Gilbert et al., 2010; Bidegain et al., 2013; Philippart et
288 al., 2012; Zhang et al., 2015), yet are nonetheless important to the ecology of this commercially
289 important stock.

290 Sea scallops in the MAB exhibit semiannual spawning with a spring spawn around May,
291 followed by a second spawn in the fall in September through November (DuPaul et al., 1989;
292 Schmitzer et al., 1991). This spawning pattern can vary annually and by scallop size, sex, and
293 water depth and is likely associated with seasonal changes in bottom water temperature (DuPaul
294 et al., 1989; Schmitzer et al., 1991). These simulations show a distinct difference in larval
295 success between releases in the spring and those in the fall, with spring (May and June) releases
296 generally being 28% less successful than those in the fall (September and October). This is
297 consistent with Chute et al. (2014), who used stable isotope analysis of scallop shells to
298 demonstrate that the adult sea scallops were primarily from fall spawns (13 out of 14 scallops

309 overall, and 7 out of 8 in MAB). In our simulations, differences in larval success between spring
300 and fall releases is largely due to differences in temperature that, in the larval model, generates
301 different larval growth rates. Using a similar model for Atlantic surfclams in the MAB, Zhang et
302 al. (2016) demonstrated seasonal differences in larval dispersal that were due to seasonal changes
303 in wind patterns and stratification.

304 Interannual variability is also evident in our simulations, with 2007 through 2009 having
305 ~5% lower larval success during August and September in comparison to other years. Observed
306 recruitment from annual stock survey programs in the MAB during those years was also
307 relatively poor (NEFSC 2014). Scallops, like many other species with high fecundity and
308 dispersive larvae, experience highly variable population abundance among years that is often
309 attributed to annually varying recruitment success (Hjort, 1914; Thorson, 1966; Levin, 2006;
310 Gaines et al., 2007). Our simulations suggest that low larval success may have been a factor
311 contributing to the low rates of recruitment observed during the 2007 through 2009 period;
312 however, other factors controlling post-settlement success (e.g. predation, disease, etc.) also
313 contribute to differences in recruit abundance among years (Ólafsson et al., 1994).

314 Larval success is also variable among the release regions. Larval sources and sinks can
315 vary over time (Munroe et al., 2014) and understanding the relative contributions of different
316 portions of a population to overall source:sink dynamics is critical to management decisions
317 about marine protected areas (Crowder et al., 2000) and fisheries (Kritzer and Sale, 2004). The
318 Long Island region tends to have the highest larval success and consistently contributes larvae
319 broadly to all other regions. Assuming these simulated results reflect the true spatial pattern of
320 connectivity in this region, the Long Island region is important not only in local larval supply but
321 also for supplying larvae regionally. Likewise, analysis of phytoplankton blooms and scallop

322 recruitment strength (NEFSC, 2014) showed that blooms are more strongly correlated to year 1
323 scallop recruit classes in Long Island than in other regions. Larval food (phytoplankton) is not
324 included as model input; however, this empirical correlation may suggest that larvae from the
325 Long Island region experience even greater success than predicted by the simulations because of
326 synchronicity between larvae and their food.

327 From a management perspective, it is important to understand the dynamics of
328 populations that are at the edge of a species' range (Hampe & Petit, 2005), especially those that
329 are larval sinks (Caddy & Gulland 1983; Cowen & Sponaugle, 2009; Kritzer and Sale, 2004).
330 Individuals at the range edge, particularly the southern end of the range, tend to be at higher risk
331 for loss (Hampe & Petit, 2005) and populations that are a sink, or a net importer of individuals
332 (Pulliam, 1988), face higher mortality risk because of their reliance on recruits from other
333 sources. It should be noted that this species is distributed over a wider area than the management
334 regions we have limited our simulations to, thus the range edges may not be entirely represented
335 here. Likewise, the overall connectivity for the species may be higher if other areas outside the
336 management areas we have included are considered. Nonetheless, the simulated larval
337 connectivity patterns from our model suggests that the Virginia Beach region contributes the
338 least larvae to other regions, and receives most of its settling larvae from regions northward.
339 Thus, this region is a sink and is positioned at the southern edge of the stock range. This could
340 have important implications in terms of vulnerability of this part of the stock (Hare et al., 2016;
341 Kleisner et al., 2017), particularly with a changing climate and uncertainty about how changes in
342 connectivity might manifest through changes to thermally-mediated larval behavior or changes
343 to regional oceanography (Mellilo et al., 2013; Rahmstorf et al., 2015; Saba et al., 2016).

344 Qualities such as how strong a larval source or sink an area is are not only important to

345 fisheries management, but are also relevant to marine spatial planning and restoration efforts.
346 Decisions about marine protected areas, such as where they should be located or how large they
347 should be, rely on understanding how populations are connected (Palumbi, 2003; Dawson et al.,
348 2006; Cowen and Sponagule 2009). Similarly, strategic planning of restoration efforts should
349 target locations that allow both survival of enhanced populations (adult shellfish) and support
350 survival of larvae spawned from these populations which requires some information about how
351 the larvae disperse both into and out of a restoration site. Simulation studies like this one can
352 provide the type of dispersal pattern information needed for marine protected area or restoration
353 planning, and can help in exploring potential evolutionary consequences of protected areas
354 (Munroe et al., 2014).

355 Direct observation and tracking marine invertebrate larvae over their entire larval
356 duration in a vast ocean remains a technical challenge (Gawarkiewicz et al., 2007) and tracking
357 even in restricted water bodies is an arduous endeavor (Arnold et al., 2005; Thomas et al., 2012).
358 Yet the importance of dispersal and connectivity to metapopulation dynamics and marine
359 management is paramount (Possingham & Roughgarden, 1990; Kerr et al., 2010; Bryan-Brown
360 et al., 2017). Although marine larvae are small, largely planktonic, and cannot overcome oceanic
361 currents *per se*, many model-based particle tracking studies show that inclusion of simulated
362 larval behavior produces patterns of dispersal and connectivity that differ from those with
363 passive particles (Metaxas & Saunders, 2009; Narváez et al. 2012b; Paris et al. 2007; Gilbert et
364 al., 2010; Zhang et al., 2015; Davies et al., 2015). As such, particle tracking in circulation models
365 is now a standard tool for assessing connectivity within metapopulations for management
366 purposes (Kritzer and Sale, 2004; Bryan-Brown et al., 2017). For example, this approach was
367 used to define stock management units that span international borders in the valuable king

368 scallop (*Pecten maximus*) fishery in Europe (Nicolle et al., 2017). Narváez et al. (2012a,b) used a
369 particle tracking simulations to estimate dispersal within an eastern oyster (*Crassostrea virginica*)
370 metapopulation in the eastern U.S. and showed that both decadal variations in river discharge
371 and tidal variability can influence the patterns of connectivity. Similarly, particle tracking
372 simulations for the dispersal of larvae of the Atlantic surfclam (*Spisula solidissima*) showed
373 seasonal patterns in connectivity that are related to regional stratification and wind stress (Zhang
374 et al. 2016). In a study examining clam dispersal and recruitment in Northern Spain, Bidegain et
375 al. (2013) incorporated both larval and settlement behavior to spawning and nursery areas of
376 interest to restoration and management agencies. These previous studies are cases in which
377 particle tracking simulation models have effectively demonstrated important mechanisms and
378 conditions under which connectivity may vary in commercial shellfish stocks.

379 The simulations used herein build on these previous studies and provide insights into
380 local, regional, seasonal, and interannual differences in larval success and population
381 connectivity for the Atlantic sea scallop, one of the most important fisheries in the U.S. (van
382 Voorhees, 2014; NEFSC, 2014). Simulated patterns of connectivity suggest that fall spawns tend
383 to produce more successful larvae, a period of poor larval success may explain a low stock
384 recruitment observed from 2007 to 2009, and the Long Island region may function as an
385 important larval source for other regions. These simulation results provide a basis for additional
386 studies that incorporate environmental conditions such as food supply and post-settlement
387 population dynamics and facilitate discussion about the management of this important fishery
388 and its vulnerability to changing environmental conditions.

389

390 **Acknowledgements**

391 This study was supported by the NOAA Fisheries and the Environment program (FATE),
392 with funds allocated through CINAR: NOAA/CINAR NA09OAR4320129 (Subaward A101070,
393 WHOI project 37022909). DM was partially supported by the USDA National Institute of Food
394 and Agriculture Hatch project accession number 1002345 through the New Jersey Agricultural
395 Experiment Station, Hatch projects NJ32115. Our gratitude to Drs. L. Jacobson, J.Hare and two
396 anonymous reviewers for their thoughtful review of earlier drafts. Drs. Julia Levin and Hernan
397 Arango provided guidance and expertise for ROMS simulations and Zhiren Wang performed the
398 coupled simulations. Oceanographic validation data were provided by Dr. Julia Levin, and
399 scallop biomass data were collected by the Northeast Fishery Science Center.

400

401 **References:**

402

403 Arnold, W.S., Hitchcock, G.L., Frischer, M.E., Wanninkhof, R., Sheng Y.P. 2005. Dispersal of
404 an introduced larval cohort in a coastal lagoon. *Limnology and Oceanography*, 50, 587-
405 597.

406

407 Beaumont, A.R., Barnes, D.A. 1992. Aspects of veliger larval growth and byssus drifting of the
408 spat of *Pecten maximus* and *Aequipecten (Chlamys) opercularis*. *ICES Journal of Marine*
409 *Science*, 49, 417-423.

410

411 Bernhardt, J.R., Leslie, H.M. 2013. Resilience to climate change in coastal marine ecosystems.
412 *Annual Review of Marine Science*, 5, 371-392.

413

414 Bidegain, G., Bárcena, J.F., García, A., Juanes, J.A., 2013. LARVAHS: predicting clam larval
415 dispersal and recruitment using habitat suitability-based particle tracking model.
416 *Ecological Modelling*, 268, 78-92.

417

418 Bryan-Brown, D.N., Brown, C.J., Hughes, J.M., Connolly, R.M. 2017. Patterns and trends in
419 marine population connectivity research. *Marine Ecology Progress Series*, 585, 243-256.

420

421 Caddy, J.F., Gulland J.A. 1983. Historical patterns of fish stocks. *Marine Policy* 7, 267-278.

422

423 Chen, S.Y., Pan, L.Y., Hong, M.J., Lee, A.C. 2012. The effects of temperature on the growth of
424 and ammonia uptake by marine microalgae. *Botanical Studies*, 53, 125-133.

425

- 426 Chia, F.S., Buckland-Nicks, J. Young, C.M. 1984. Locomotion of marine invertebrate larvae: a
427 review. *Canadian Journal of Zoology* 62, 1205-1222.
428
- 429 Chute, A.S., Wainright, S.C., Hart, D.R. 2012. Timing of shell ring formation and patterns of
430 shell growth in the sea scallop *Placopecten magellanicus* based on stable oxygen isotopes.
431 *Journal of Shellfish Research*, 31, 649-662.
432
- 433 Cowen, R., Sponaugle, S. 2009. Larval dispersal and marine population connectivity. *Annual*
434 *Review of Marine Science* 1, 443-466.
435
- 436 Crowder L, Lyman S, Figueira W, Priddy J. 2000. Source-sink population dynamics and the
437 problem of siting marine reserves. *Bulletin of Marine Science* 66, 799–820.
438
- 439 Culliney, J. L., 1974. Larval development of the giant scallop *Placopecten magellanicus*
440 (Gmelin). *The Biological Bulletin*, 147, 321-332
441
- 442 Dawson, M., Grosberg, R., Botsford, L. 2006. Connectivity in marine protected areas. *Science*,
443 313, 43-44.
444
- 445 Davies, K.T.A., Gentleman, W.C., DiBacco, C., Johnson, C.L. 2015. Fisheries closed areas
446 strengthen scallop larval settlement and connectivity among closed areas and across
447 international open fishing grounds: a model study. *Environmental Management*, 56, 587-
448 602.
449
- 450 Gaines S.D., Gaylord B., Gerber L.R., Hastings A., Kinlan B.P. 2007. Connecting places: The
451 ecological consequences of dispersal in the sea. *Oceanography*, 20, 90–99.
452
- 453 Gallagher, S.M., Manuel J.L., Manning D.A., O’Dor, R. 1996. Ontogenetic changes in the
454 vertical distribution of giant scallop larvae, *Placopecten magellanicus*, in 9-m deep
455 mesocosms as a function of light, food, and temperature stratification. *Marine Biology*,
456 124, 679-692.
457
- 458 Gawarkiewicz, G., Monismith, S., Largier, J. 2007. Observing larval transport processes
459 affecting population connectivity. *Oceanography*, 20, 14.
460
- 461 Gilbert, C.S., Gentleman, W.C., Johnson, C.L., DiBacco, C., Pringle, J.M., Chen, C. 2010.
462 Modeling dispersal of sea scallop (*Placopecten magellanicus*) larvae on Georges Bank:
463 The influence of depth-distribution, planktonic duration and spawning seasonality.
464 *Progress in Oceanography*, 87, 37-48.
465
- 466 Gouda, R., Kenchington, E., Hatcher, B., Vercaemer, B. 2006. Effects of locally isolated micro-
467 phytoplankton diets on growth and survival of sea scallop (*Placopecten magellanicus*)
468 larvae. *Aquaculture*, 259, 169-180.
469
- 470 Hampe, A. Petit, R. J. 2005. Conserving biodiversity under climate change: The rear edge
471 matters. *Ecology Letters*, 8, 461–467.

472
473 Hart, D.R. 2003. Yield- and biomass- per-recruit analysis for rotational fisheries, with an
474 application to Atlantic sea scallop (*Placopecten magellanicus*). Fishery Bulletin, 101, 44-
475 57.
476
477 Hart, D.R. 2006. Effects of sea stars and crabs on sea scallop *Placopecten magellanicus*
478 recruitment in the Mid-Atlantic Bight (USA). Marine Ecology Progress Series, 306,
479 209–221.
480
481 Hart, D. R. 2013. Quantifying the tradeoff between precaution and yield in fishery reference
482 points. ICES Journal of Marine Science, 70, 591–603.
483
484 Hart, D.R., Rago, P.J.. 2006. Long-term dynamics of U.S. sea scallop (*Placopecten magellanicus*)
485 populations. North American Journal of Fisheries Management, 26, 490-501.
486
487 Hart D.R, Shank B. 2011. Mortality of sea scallops *Placopecten magellanicus* in the Mid-
488 Atlantic Bight: comment on Stokesbury *et al.* (2011). Marine Ecology Progress Series,
489 443, 293-297.
490
491 Hare, J.A., Morrison, W.E., Nelson, M.W., Stachura, M.M., Teeters, E.J., Griffis, R.B.,
492 Alexander, M.A., Scott, J.D., Alade, L., Bell, R.J., Chute, A.S. 2016. A vulnerability
493 assessment of fish and invertebrates to climate change on the Northeast US continental
494 shelf. PloS One, 11, p.e0146756.
495
496 Hjort, J. 1914. Fluctuations in the great fisheries of northern Europe, viewed in the light of
497 biological research. Conseil Permanent International Pour l'Exploration de la Mer:
498 Rapports et Procès-Verbaux des Réunions, vol 20, 228 pp.
499
500 Hurley, G.V., Tremblay, M.J., Couturier, C. 1986. Daily growth increments in the shells of larval
501 sea scallops (*Placopecten magellanicus*). Northwest Atlantic Fisheries Organization
502 (NAFO) Science Council Research Document 86/99. 11 p.
503
504 Hurley, G.V., Tremblay, M.J., Couturier, C. 1987. Age estimation of sea scallop larvae
505 (*Placopecten magellanicus*) from daily growth lines on shells. Journal of Northwest
506 Atlantic Fishery Science, 7, 123-129.
507
508 Kerr, L., Cadrin, S.X., Secor, D.H. 2010. Simulation modelling as a tool for examining the
509 consequences of spatial structure and connectivity on local and regional population
510 dynamics. ICES Journal of Marine Science, 67, 1631-1639.
511
512 Kim, C.K., Park, K., Powers, S.P., Graham, W.M., Bayha, K.M. 2010. Oyster larval transport in
513 coastal Alabama: dominance of physical transport over biological behavior in a shallow
514 estuary. Journal of Geophysical Research: Oceans, 115(C10).
515

516 Kleisner, K.M., Fogarty, M.J., McGee, S., Hare, J.A., Moret, S., Perretti, C.T., Saba, V.S. 2017.
517 Marine species distribution shifts on the US northeast continental shelf under continued
518 ocean warming. *Progress in Oceanography* 153, 24-36.
519

520 Kritzer, J.P., Sale, P.F. 2004. Metapopulation ecology in the sea: from Levins' model to marine
521 ecology and fisheries science. *Fish and Fisheries*, 5, 131-140.
522

523 Lavens, P., Sorgeloos, P. 1996. Manual on the production and use of live food for aquaculture
524 (No. 361). Food and Agriculture Organization (FAO).
525 <http://www.fao.org/docrep/003/w3732e/w3732e07.htm>
526

527 Lentz, S.J. 2008. Observations and a model of the mean circulation over the Middle Atlantic
528 Bight continental shelf. *Journal of Physical Oceanography*, 38, 1203-1222. doi:
529 10.1175/2007JPO3768.1.
530

531 Levin, L.A. 2006. Recent progress in understanding larval dispersal: new directions and
532 digressions. *Integrative & Comparative Biology* 46, 282-297.
533

534 Manuel, J.L., Dadswell, M.J. 1991. Swimming behavior of juvenile giant scallop, *Placopecten*
535 *magellanicus*, in relation to size and temperature. *Canadian Journal of Zoology*, 69, 2250-
536 2254.
537

538 Manuel, J.L., Dadswell, M.J. 1993. Swimming of juvenile sea scallops, *Placopecten*
539 *magellanicus* (Gmelin): a minimum size for effective swimming? *Journal of*
540 *Experimental Marine Biology and Ecology*, 174, 137-175.
541

542 Manuel, J.L., Gallagher, S.M., Pearce, C.M., Manning, D.A., O'Dor, R.K. 1996. Veligers from
543 different populations of sea scallop *Placopecten magellanicus* have different vertical
544 migration patterns. *Marine Ecology Progress Series*, 142, 147-163.
545

546 Manuel, J.L., Pearce, C.M., Manning, D.A., O'Dor, R.K. 2000. The response of sea scallop
547 (*Placopecten magellanicus*) veligers to a weak thermocline in 9-m deep mesocosms.
548 *Marine Biology*, 137, 169-175.
549

550 Marchesiello, P., McWilliams, J.C., Shepetchkin, A. 2001. Open boundary conditions for long-
551 term integration of regional ocean models, *Ocean Modelling*, 3, 1-20.
552

553 Melillo, J.M., Richmond, T.C., Yohe, G.W. editors. 2014: *Climate Change Impacts in the United*
554 *States: The Third National Climate Assessment*. U.S. Global Change Research Program,
555 841 pp.
556

557 Mellor, G.L., Yamada, T. 1982. Development of a turbulent closure model for geophysical fluid
558 problems. *Reviews of Geophysics and Space Physics*, 20, 851-875.
559

- 560 Metaxas A. 2001. Behaviour in flow: perspectives on the distribution and dispersion of
561 meroplanktonic larvae in the water column. Canadian Journal of Fisheries and Aquatic
562 Science 58, 86-98. doi:10.1139/cjfas-58-1-86.
563
- 564 Metaxas A., Saunders M. 2009. Quantifying the "bio-" components in biophysical models of
565 larval transport in marine benthic invertebrates: advances and pitfalls. The Biological
566 Bulletin, 216, 257-272.
567
- 568 Munroe, D.M., Noda, T. 2010. Physical and biological factors contributing to changes in the
569 relative importance of recruitment to population dynamics in open populations. Marine
570 Ecology Progress Series, 412: 151-162. DOI:10.3354/meps08712
571
- 572 Munroe, D., Klinck, J., Hofmann, E., Powell, E.N. 2012. The role of larval dispersal in
573 metapopulation gene flow: local population dynamics matter. Journal of Marine
574 Research, 70, 441-467. DOI: 10.1357/002224012802851869.
575
- 576 Munroe, D., Klinck, J., Hofmann, E., Powell, E.N. 2013. How do shellfisheries influence genetic
577 connectivity in metapopulations? A modeling study examining the role of lower size
578 limits in oyster fisheries. Canadian Journal of Fisheries and Aquatic Sciences, 70, 1813-
579 1828, DOI: 10.1139/cjfas-2013-0089
580
- 581 Munroe, D., Hofmann, E., Klinck, J., Powell, E., Ford, S.E. 2015. Consequences of
582 asymmetric disease pressure and larval dispersal on the evolution of disease resistance; a
583 metapopulation modeling study with oysters. Marine Ecology Progress Series, 531, 221-
584 239. [doi:10.3354/meps11349](https://doi.org/10.3354/meps11349)
585
- 586 Munroe, D., Klinck, J., Hofmann, E., Powell, E.N.P. 2014. A modeling study of metapopulation
587 genetic connectivity in Delaware Bay oysters and the role of marine protected areas.
588 Aquatic Conservation, 24, 645-666. [DOI: 10.1002/aqc.2400](https://doi.org/10.1002/aqc.2400)
589
- 590 Narváez, D.A., Klinck, J.M., Powell, E.N., Hofmann, E.E., Wilkin, J., Haidvogel, D.B. 2012a.
591 Modeling the dispersal of eastern oyster (*Crassostrea virginica*) larvae in Delaware Bay.
592 Journal of Marine Research, 70, 381-409.
593
- 594 Narváez, D.A., Klinck, J.M., Powell, E.N., Hofmann, E.E., Wilkin, J., Haidvogel, D.B. 2012b.
595 Circulation and behavior controls on dispersal of eastern oyster (*Crassostrea virginica*)
596 larvae in Delaware Bay. Journal of Marine Research, 70, 2-3.
597
- 598 National Marine Fisheries Service (NMFS). 2017. Fisheries of the United States, 2016. U.S.
599 Department of Commerce, NOAA Current Fishery Statistics No. 2016. Available at:
600 <https://www.st.nmfs.noaa.gov/commercial-fisheries/fus/fus16/index>
601
- 602 Nicolle, A., Moitié, R., Ogor, J., Dumas, F., Foveau, A., Foucher, E., Thiébaud, E. 2017.
603 Modelling larval dispersal of *Pecten maximus* in the English Channel: a tool for the
604 spatial management of the stocks. ICES Journal of Marine Science, 74, 1812-1825.
605

606 Northeast Fisheries Science Center [NEFSC], 2014. 59th Northeast Regional Stock Assessment
607 Workshop (59th SAW) Assessment Report. U.S. Department of Commerce, Northeast
608 Fisheries Science Center Reference Document 14-09
609

610 North, E.W., Schlag, Z., Hood, R.R., Li, M., Zhong, L., Gross, T., Kennedy, V. S. 2008. Vertical
611 swimming behavior influences the dispersal of simulated oyster larvae in a coupled
612 particle-tracking and hydrodynamic model of Chesapeake Bay. *Marine Ecology Progress
613 Series*, 359, 99-115.
614

615 Ólafsson, E.B., Peterson, C.H., Ambrose, W.G. 1994. Does recruitment limitation structure
616 populations and communities of macro-invertebrates in marine soft sediments: the
617 relative significance of presettlement and postsettlement processes. *Oceanography and
618 Marine Biology*, 32, 65-109.
619

620 Palumbi, S.R. 2003. Population genetics, demographic connectivity, and the design of marine
621 reserves. *Ecological Applications*. 13, 146-158.
622

623 Pearce, C.M., Manuel, J.L., Gallager, S.M., Manning, D.A., O'Dor, R.K., Bourget, E. 2004.
624 Depth and timing of settlement of veligers from different populations of giant scallop,
625 *Placopecten magellanicus* (Gmelin), in thermally stratified mesocosms. *Journal of
626 Experimental Marine Biology and Ecology*, 312, 187-214.
627

628 Pernet, F., Tremblay, R., Bourget, E. 2003. Biochemical indicator of sea scallop (*Placopecten
629 magellanicus*) quality based on lipid class composition. Part II: Larval growth,
630 competency and settlement. *Journal of Shellfish Research*, 22, 377-388.
631

632 Peterson, C.H., Summerson, H.C., Luettich Jr., R.A. 1996. Response of bay scallops to spawner
633 transplants: a test of recruitment limitation. *Marine Ecology Progress Series* 132, 93-107.
634

635 Philippart, C.J.M., Amaral, A., Asmus, R., van Bleijswijk, J., Bremner, J., Buchholz, F.,
636 Cabanellas-Reboredo, M., Catarino, D., Cattrijsse, A., Charles, F., Comtet, T., Cunha, A.,
637 Deudero, S., Duchêne, J-C., Fraschetti, S., Gentil, F., Gittenberger, A., Guizien, K.,
638 Gonçalves, J.M., Guarnieri, G., Hendriks, I., Hussel, B., Pinheiro Vieira, R., Reijnen,
639 B.T., Sampaio, I., Serrao, E., Sousa Pinto, I., Thiebaut, E., Viard, F., Zuur, A.F. 20012.
640 Spatial synchronies in the seasonal occurrence of larvae of oysters (*Crassostrea gigas*)
641 and mussels (*Mytilus edulis/galloprovincialis*) in European coastal waters. *Estuarine,
642 Coastal and Shelf Science*, 108, 52-63.
643

644 Pineda, J., Hare, J.A., Sponaugle, S. 2007. Larval transport and dispersal in the coastal ocean and
645 consequences for population connectivity. *Oceanography*, 20, 22-39.
646

647 Possingham, H.P., Roughgarden, J. 1990. Spatial population-dynamics of a marine organism
648 with a complex life-cycle, *Ecology*, 71, 973-985.
649

650 Pulliam, H.R. 1988. Sources, sinks, and population regulation. *American Naturalist*, 132, 652–
651 661.

652
653 Rahmstorf, S., Feulner, G., Mann, M. E., Robinson, A., Rutherford, S., Schaffernicht, E. J. 2015.
654 Exceptional twentieth-century slowdown in Atlantic Ocean overturning circulation.
655 Nature Climate Change, 5, 475-480.
656
657 Saba, V.S., Griffies, S.M., Anderson, W.G., Winton, M., Alexander, M.A., Delworth, T.L., Hare,
658 J.A., Harrison, M.J., Rosati, A., Vecchi, G.A., Zhang, R. 2015. Enhanced warming of the
659 Northwest Atlantic Ocean under climate change. Journal of Geophysical Research:
660 Oceans, doi:10.1002/2015JC011346.
661
662 Scheltema, R.S. 1971. Larval dispersal as a means of genetic exchange between geographically
663 separated populations of shallow-water benthic marine gastropods. The Biological
664 Bulletin, 140, 284-322.
665
666 Shank, B.V., Hart, D.R., Friedland, K.D. 2012. Post-settlement predation by sea stars and crabs
667 on the sea scallop in the Mid-Atlantic Bight. Marine Ecology Progress Series, 468, 161-
668 177.
669
670 Shchepetkin, A.F., McWilliams, J.C. 2005. The Regional Ocean Modeling System: a split-
671 explicit, free-surface, topography-following coordinate oceanic model. Ocean Modelling,
672 9, 347-404.
673
674 Shank, B.V., Hart, D.R., Freidland, K.D. 2012. Post-settlement predation by sea stars and crabs
675 on the sea scallop (*Placopecten magellanicus*) in the Mid Atlantic Bight. Marine Ecology
676 Progress Series, 468, 161-177.
677
678 Strathmann R.R., Hughes T.P., Kuris A.M., Lindeman, K.C., Morgan, S.G., Pandolfi, J.M.,
679 Warner, R.R. 2002. Evolution of local recruitment and its consequences for marine
680 populations. Bulletin of Marine Science, 70, S377-S396.
681
682 Tettelbach, S.T., Peterson, B.J., Carroll, J.M., Hughes, S.W.T., Bonal, D.M., Weinstock, A.J.,
683 Europe, J.R., Furman, B.T., Smith, C.F. 2013. Priming the larval pump: resurgence of
684 bay scallop recruitment following initiation of intensive restoration efforts, Marine
685 Ecology Progress Series, 478, 153-172.
686
687 Thomas, Y., Garen, P., Bennett, A., le Pennec, M., Clavier, J. 2012. Multi-scale distribution and
688 dynamics of bivalve larvae in a deep atoll lagoon (Ahe, French Polynesia). Marine
689 Pollution Bulletin, 65, 453-462.
690
691 Thorson, G. 1966. Some factors influencing the recruitment and establishment of marine benthic
692 communities. Netherlands Journal of Sea Research, 3, 267-293.
693
694 Tian, R., Chen, C., Stokesbury, K.D.E., Rothschild, B.J., Xu, Q., Hu, S., Marino, M.C.II. 2009.
695 Modeling exploration of the connectivity between sea scallop populations in the Middle
696 Atlantic Bight and over Georges Bank. Marine Ecology Progress Series, 380, 147-160.
697

698 Tremblay, M.J., Loder, M.W., Werner, F.E., Naimie, C.E., Page, F.H., Sinclair, M.M. 1994.
699 Drift of sea scallop larvae *Placopecten magellanicus* on Georges Bank: a model study of
700 the roles of mean advection, larval behavior and larval origin. Deep Sea Research Part II:
701 Topical Studies in Oceanography, 41, 7-49.
702

703 Tremblay, M.J., Sinclair, M.M. 1988. The vertical and horizontal distribution of sea scallop
704 (*Placopecten magellanicus*) larvae in the Bay of Fundy in 1984 and 1985. Journal of
705 Northwest Atlantic Fishery Science, 8, 43-53.
706

707 Tremblay, M.J., Sinclair, M.M. 1990. Sea scallop larvae *Placopecten magellanicus* on Georges
708 Bank: vertical distribution in relation to water column stratification and food. Marine
709 Ecology Progress Series., 61, 1- 15.
710

711 Umlauf, L., Burchard, H. 2003. A generic length-scale equation for geophysical turbulence
712 models, Journal of Marine Research, 61, 235-265.
713

714 Van Voorhees, D. (Editor). 2014. Fisheries of the United States, 2013. NMFS Office of
715 Science and Technology, Fisheries Statistics Division, Silver Spring, Maryland, August
716 2014.
717

718 Warner, J.C., Sherwood, C.R., Arango, H.G., Signell, R.P. 2005a. Performance of four
719 turbulence closure methods implemented using a generic length scale method, Ocean
720 Modelling, 8, 81-113.
721

722 Warner, J.C., Geyer, W.R., Lerczak, J.A. 2005b. Numerical modeling of an estuary: a
723 comprehensive skill assessment. Journal of Geophysical Research, 110, 1-13.
724

725 Wilkin, J., Hunter, E. 2013. An assessment of the skill of real-time models of Middle Atlantic
726 Bight continental shelf circulation. Journal of Geophysical Research: Oceans, 118
727 doi:10.1002/jgrc.20223.
728

729 Xue, H., Incze, L., Xu, D., Wolff, N., Pettigrew, N. 2008. Connectivity of lobster populations in
730 the coastal Gulf of Maine: Part I: circulation and larval transport potential. Ecological
731 Modelling, 210, 193-211.
732

733 Zhang, P., Haidvogel, D., Powell, E., Klinck, J., Mann, R., Castruccio, F., Munroe, D. 2015. A
734 coupled physical and biological model of larval connectivity in Atlantic surfclams along
735 the Middle Atlantic Bight. Part I: model development and description. Estuarine Coastal
736 and Shelf Science. 153, 38-53. [doi:10.1016/j.ecss.2014.11.033](https://doi.org/10.1016/j.ecss.2014.11.033)
737

738 Zhang, X., Munroe, D., Haidvogel, D., Powell, E.N. 2016. Atlantic surfclam connectivity within
739 the Middle Atlantic Bight: mechanisms underlying variation in larval transport and
740 settlement. Estuarine, Coastal and Shelf Science, 173, 65-78.
741

742

743 **Figure Captions:**

744

745 **Figure 1.** Model domain (*i.e.*, 68–77° W, 33.8–42° N), with an example larval release for a
746 single day in 2006 overlaid; release locations indicated by transparent dots. The regions shown
747 are the delineations of regions used in calculations of connectivity and reflect federal
748 management regions used for this species (NEFSC, 2014).

749

750 **Figure 2:** Average larval success for each release period, grouped by ‘E’ for early (1st and 6th),
751 ‘M’ for mid (11th and 16th) and ‘L’ for late (21st and 26th) days of each month (y-axis) and region
752 (x-axis). Each panel shows the average larval success for a given year (as labeled), with the panel
753 in the bottom right showing the mean larval success averaged across all years. The number in the
754 center of the colored squares are the rounded % settlement success. White squares with no
755 number indicate that no larvae released during that period/region combination were successful.
756 Region names are abbreviated as follows: Long Island: LI; New York Bight: NYB; Delmarva:
757 DMV; and Virginia Beach: VB.

758

759

760 **Figure 3:** Average larval growth rate across the entire larval duration for each larval release
761 period, grouped by ‘E’ for early (1st and 6th), ‘M’ for mid (11th and 16th) and ‘L’ for late (21st and
762 26th) days of each month (y-axis) and region (x-axis). Each panel shows the average growth rate
763 of successful larval for a given year (as labeled), with the panel in the bottom right showing the
764 mean growth rate of successful larvae averaged across all years. White squares indicate that no
765 larvae released during that period/region combination were successful. Region names are

766 abbreviated as follows: Long Island: LI; New York Bight: NYB; Delmarva: DMV; and Virginia
767 Beach: VB.

768

769 **Figure 4:** Median temperature a released group of larvae experiences and the median growth rate
770 over the same group's pelagic duration. Only larvae that are successful are shown, and each point
771 represents the median over all larvae for a given release day and year. Release months are shown
772 separately using distinct symbols.

773

774 **Figure 5:** Connectivity matrices among scallop regions, shown as percent of larvae successfully
775 dispersing from the starting region to the settling region for all larvae released in a given year.
776 The panel in the bottom right shows the average connectivity pattern across all releases for all
777 years. Release regions are listed on the y-axis, destination regions listed along the x-axis. The
778 shading within each grid cell is the proportion of all larvae released from a given region that
779 successfully end in the given destination region. Region names are abbreviated as follows: Block
780 Island: BI; Long Island: LI; New York Bight: NYB; Delmarva: DMV; and Virginia Beach: VB.

781

782 **Figure 6:** Connectivity matrices among scallop regions, shown as percent of larvae successfully
783 dispersing from the starting region to the settling region for all larvae released in September.
784 Each panel shows the total larval connectivity over all releases in September for a given year (as
785 labeled), with the panel in the bottom right showing the average connectivity pattern across all
786 September releases for all years. Region names are abbreviated as follows: Block Island: BI;
787 Long Island: LI; New York Bight: NYB; Delmarva: DMV; and Virginia Beach: VB.

788

795 Tables:

796

797 Table 1. Parameters for simulating growth and swimming of sea scallop larvae.

Par.	Unit	Value	Definition
Gr_0	$\mu m \text{ day}^{-1}$	3.9	Initial basic larval growth rate, set as linear rate observed at 13°C.
Gr_1	1°C	0.069	Rate of increase of growth rate with temperature.
T_1	°C	13	Base temperature for growth.
T_2	°C	17	Optimum growth temperature.
T_3	°C	19	Highest temperature above which growth is zero.
Fu_{s0}		0.5	Initial upward swimming time fraction.
Sk_0		2.22×10^{-4}	Leading coefficient of sinking speed function.
Sk_1		1.744	Exponent of the power function of sinking speed.
Us_0	mm s ⁻¹	-0.381	Coefficients of the quadratic function giving upward swimming speed as a function of larval length.
Us_1	mm s ⁻¹ μm ⁻¹	9.262×10^{-3}	
Us_2	mm s ⁻¹ μm ⁻²	-2.692×10^{-5}	
Ds_0	mm s ⁻¹	-0.561	Coefficients of the quadratic function giving downward swimming speed as a function of larval length.
Ds_1	mm s ⁻¹ μm ⁻¹	1.749×10^{-2}	
Ds_2	mm s ⁻¹ μm ⁻²	-6.538×10^{-5}	
T_{us1}	°C	16.5	Temperature at which half of swimming time is spent in swimming upward.
T_{us2}	°C	0.9	Temperature coefficient that controls the fraction of swimming time spent swimming upward.
D_i	μm	75	Initial larvae size at 1.5 days old.
D_{s1}	μm	240	Minimum settlement size, corresponds to the size at which larvae begin to move downward to the bottom.
D_{s2}	μm	270	Maximum settlement size.

798

799

800

801

802 **Table 2.** Larval release strategies for each simulated year. The table below shows the total
803 number of larvae released on each year over 36 total daily releases, occurring at 00:00, 04:08,
804 and 08:17 daily on day 1, 6, 11, 16, 21 and 26 of May-October each year. In each year, the
805 number of larvae are scaled spatially over the release points within each region (Figure 1)
806 relative to the spatially explicit gonad biomass estimated from annual stock survey sampling
807 (NEFSC, 2014).

808

Region\Year	2006	2007	2008	2009	2010	2011	2012
Long Island	32693	32688	32866	32599	32686	32416	32735
NY Bight	31050	31660	31680	31754	31948	31643	31694
Delmarva	14658	14709	14632	14727	14517	14602	14604
Virginia Beach	3857	3823	3748	3769	3491	3730	3811

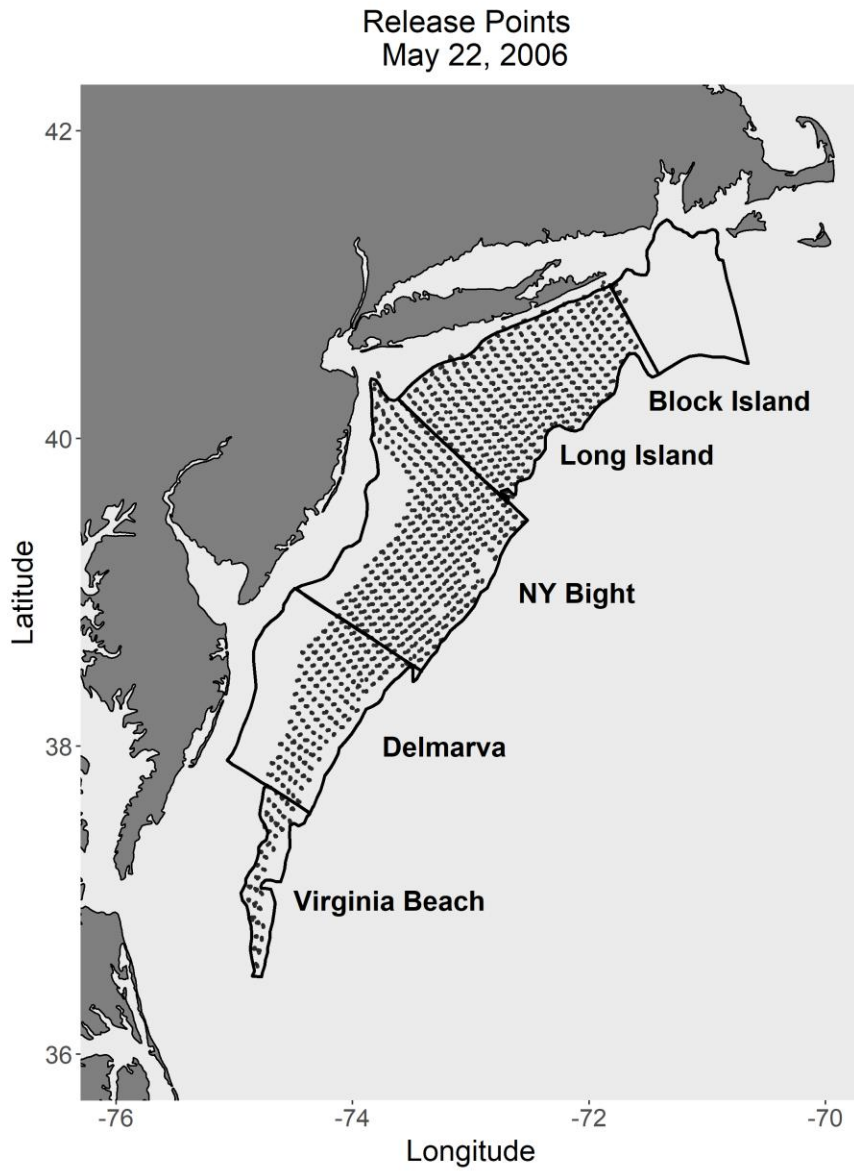
809

810

811

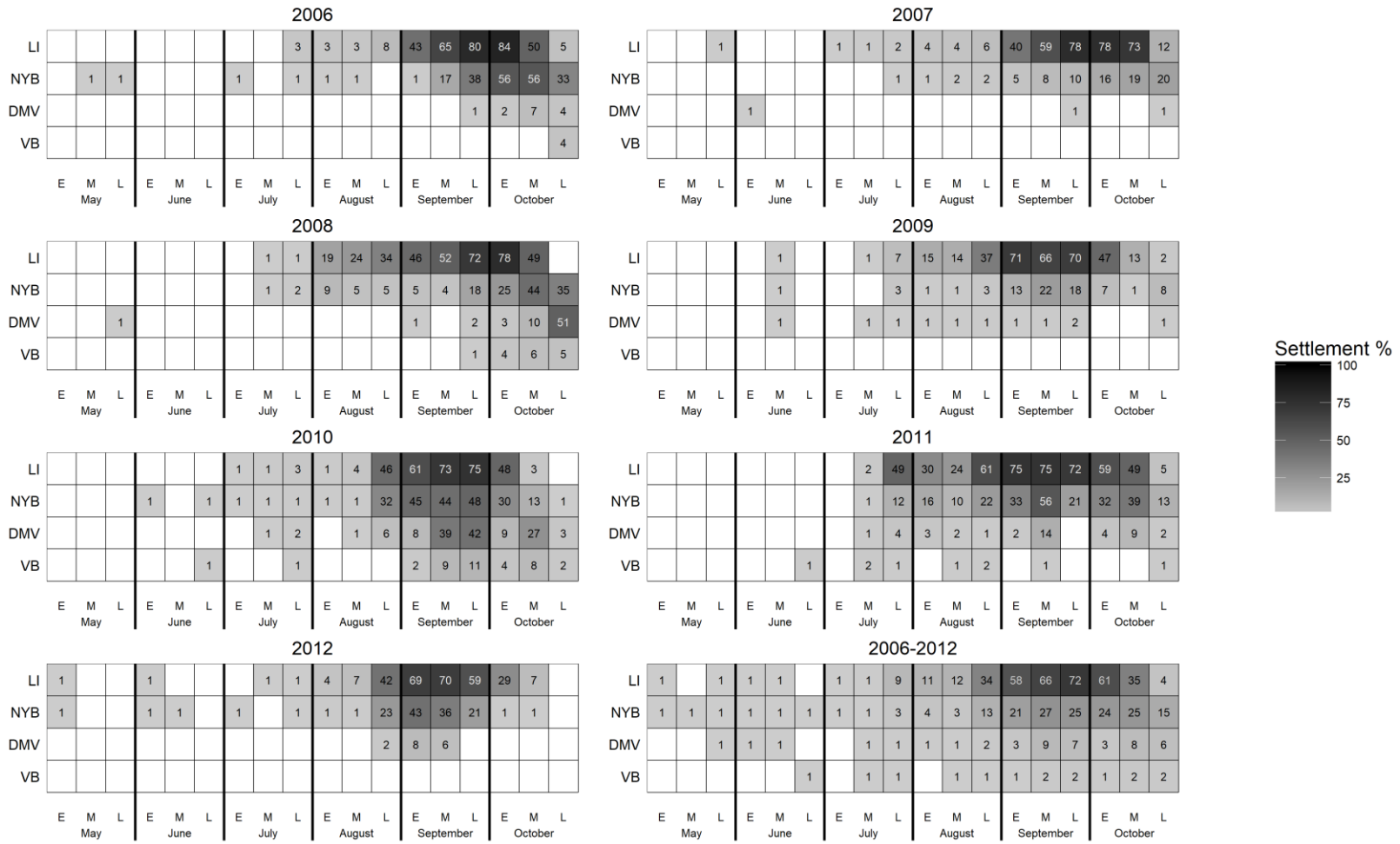
812 **Figures:**

813 Figure 1:



814

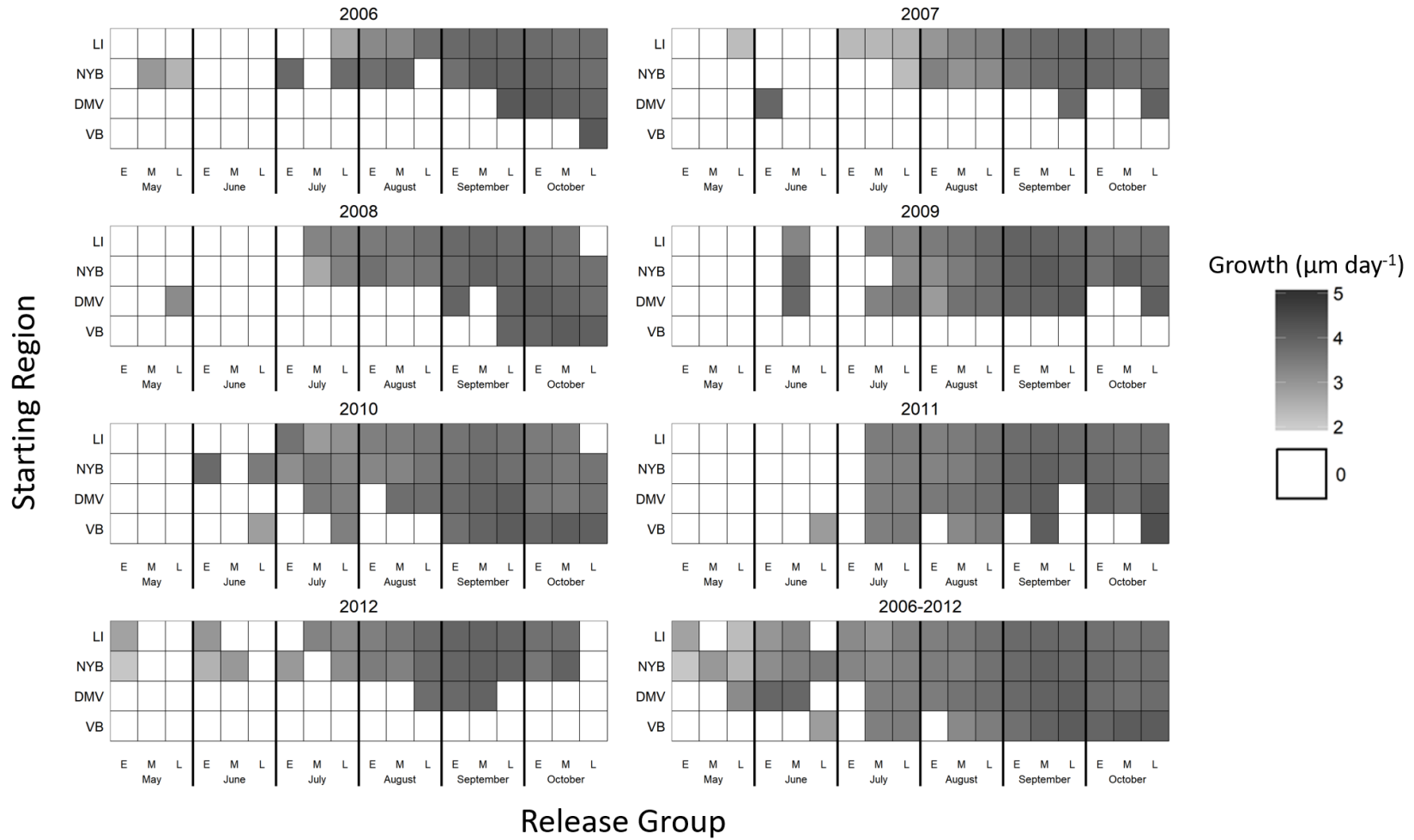
815 Figure 2:
 816
 817



818

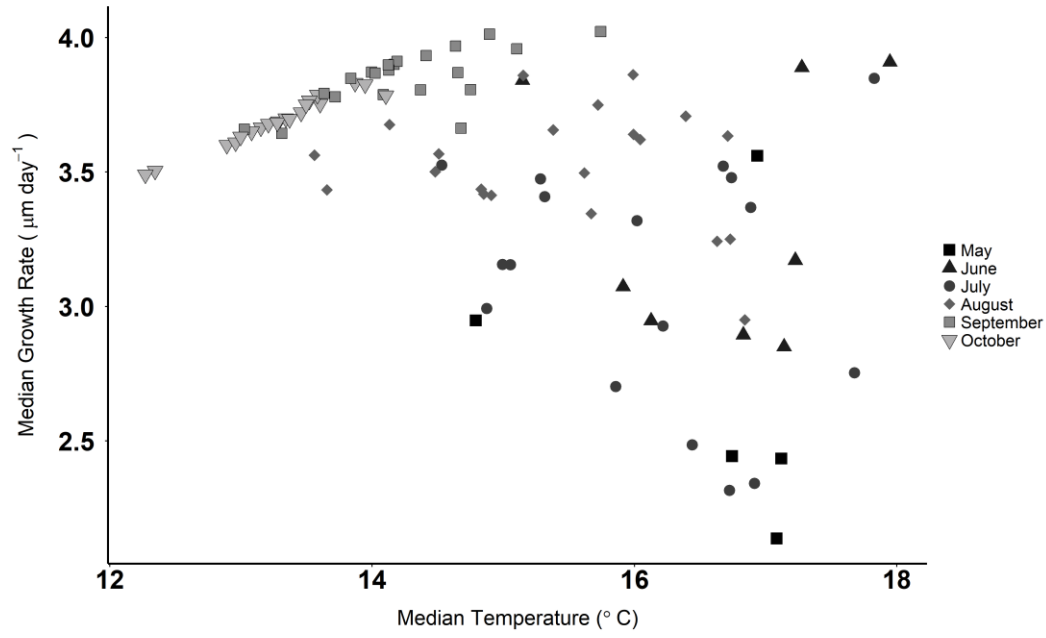
819 Figure 3:

820



821

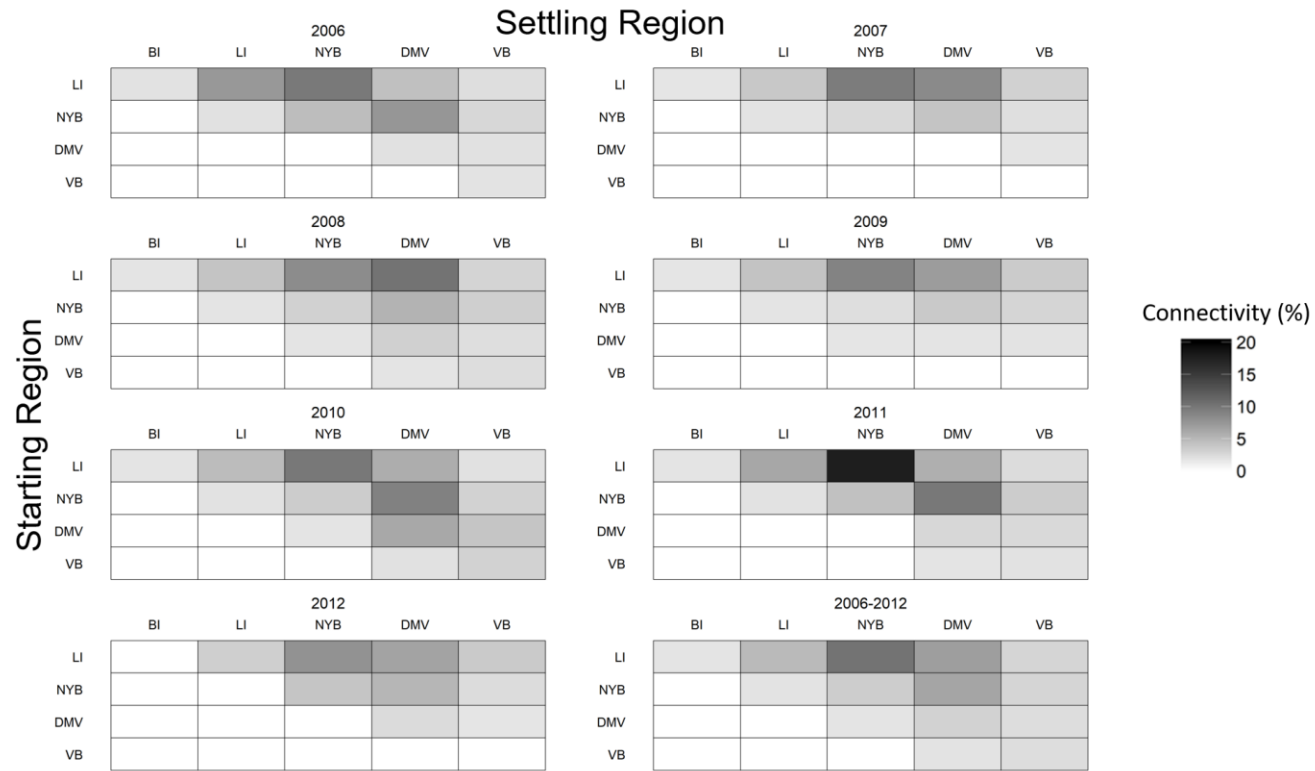
822 Figure 4:



823

824

825 Figure 5:

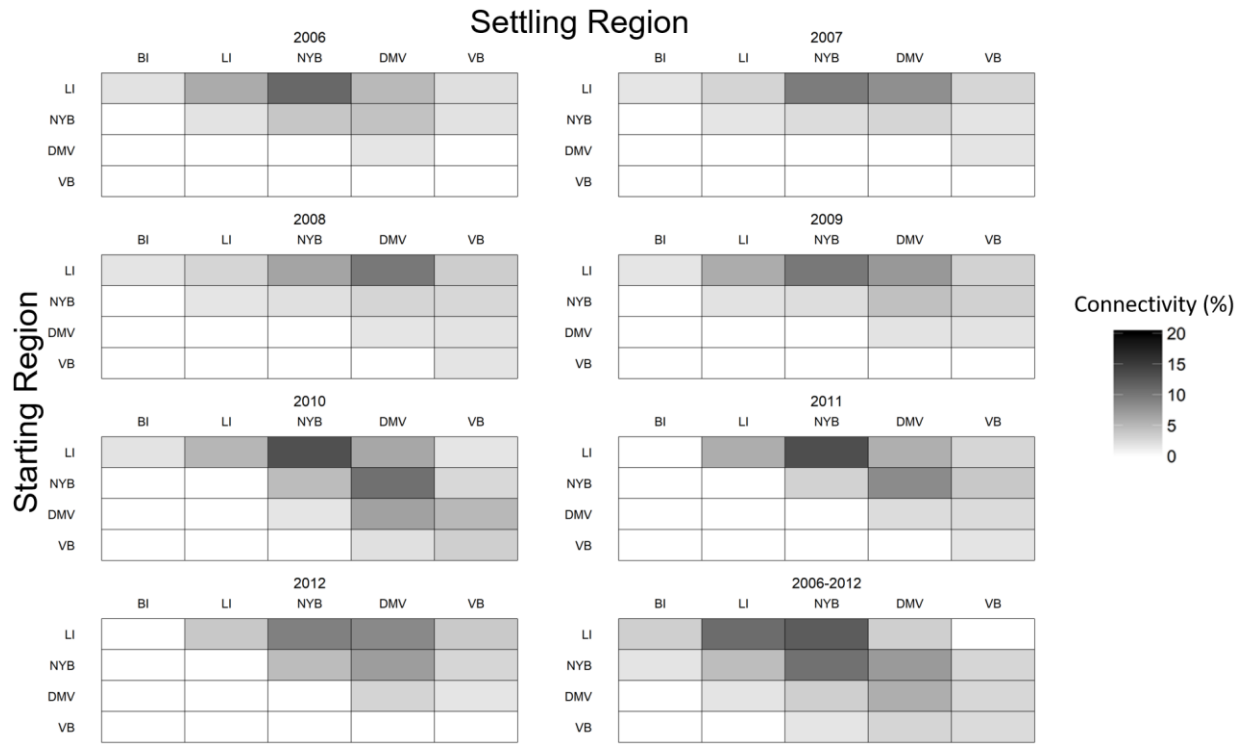


826

827

828

829 Figure 6:



830